Trends in Electronic Structure and Redox Energetics for Early-Actinide Pentamethylcyclopentadienyl Complexes

David E. Morris,* Ryan E. Da Re, Kimberly C. Jantunen, Ingrid Castro-Rodriguez, and Jaqueline L. Kiplinger*

Chemistry Division and the Glenn T. Seaborg Institute for Transactinium Science, Los Alamos National Laboratory, Los Alamos, New Mexico 87545

Received May 21, 2004

Detailed cyclic voltammetric and UV−visible−near-infrared electronic absorption spectral data have been obtained for a series of pentamethylcyclopentadienyl complexes of uranium(IV) and thorium(IV) of the general formula $(C_5Me_5)_2An(L_1)(L_2)$, where L_1, L_2 = Cl, SO_3CF_3, CH_3, CH_2Ph, imido (=N-2,4,6-$^tBu_3C_6H_2$), hydrazonato (η^2(*N*,*N*′)-RNN=CPh_2; R = CH_3, CH_2-Ph, Ph), ketimido (−N=C(Ph)(R); R = CH_3, CH_2Ph, Ph) ligands, and for the hexavalent uranium bis(imido) complex $(C_5Me_5)_2U(=NPh)_2$. The electrochemical and spectroscopic behavior of the tetravalent uranium complexes falls cleanly into distinct categories based on the nature of L_1 and L_2. If both ligands are simple σ-donors (Cl, SO_3CF_3, CH_3, CH_2Ph), a reversible U(IV)/U(III) voltammetric wave is the only metal-based process observed, and it occurs between ∼−1.8 and −2.6 V vs $[(C_5H_5)_2Fe]^{+/0}$. If either L_1 or L_2 is a nitrogen-donor ligand (imido, hydrazonato, ketimido), then both a U(IV)/U(III) reduction wave and a U(V)/U(IV) oxidation wave are observed. The reduction step occurs in the same potential region as for the σ-donor complexes, and the oxidation wave occurs in the range from ∼+0.2 to −0.7 V vs $[(C_5H_5)_2Fe]^{+/0}$. This oxidation wave is reversible, indicating that the unusual pentavalent uranium oxidation state is kinetically stable on a voltammetric time scale, and the potential of the oxidation step indicates that the pentavalent state is thermodynamically stabilized from interaction with the nitrogen-donor ligand(s). The separation between reduction and oxidation processes in these nitrogen-donor complexes remains nearly constant over the series of eight complexes, with an average value of 2.09 V. Additional ligand-based redox processes are also observed and assigned on the basis of the existence of corresponding voltammetric waves in the Th(IV) complexes and other cyclopentadiene complexes. The electronic absorption spectra for all U(IV) complexes are comprised of two distinct regions: a lower energy region (E < 15 000 cm^{-1}) containing the narrow f−f transitions arising from within the 5f orbital manifold and a higher energy region (E > 15 000 cm^{-1}) containing broad, unstructured, or poorly structured bands derived from both metal-localized 5f−6d transitions and molecular-based transitions including ligand-localized and metal-to-ligand charge-transfer transitions. A definite trend in intensities of these transitions is observed, depending on the nature of L_1 and L_2. If L_1 and L_2 are both simple σ-donor ligands, the f−f transition intensities are relatively weak (molar absorptivity $\epsilon \approx 10-80$ M^{-1} cm^{-1}), consistent with observations for most classical coordination complexes of 5f^2 electronic configuration, and the broad, higher energy bands have ϵ values in the 3000−5000 M^{-1} cm^{-1} range. If L_1 and/or L_2 is a hydrazonato ligand, the f−f transition intensities increase to ∼30−120 M^{-1} cm^{-1} and the broad, higher energy bands develop significantly greater intensities ($\epsilon \approx$ 15 000−20 000 M^{-1} cm^{-1}). Finally, for the imido and ketimido complexes of U(IV), the f−f transition intensities increase to ∼50−400 M^{-1} cm^{-1}, and the broad, higher energy bands continue to carry substantial intensity ($\epsilon \approx$ 10 000−15 000 M^{-1} cm^{-1}) while also extending to lower energy. This interesting trend in f−f transition intensity is interpreted in the context of an intensity-stealing mechanism from the charge-transfer excited states that reflects an enhanced degree of covalent interaction between the actinide metal center and L_1/L_2 for the nitrogen-donor ligand systems.

Introduction

Much of our current understanding of the influence of coordination environment on electronic structure and redox potentials in the light actinide elements is derived from classical coordination compounds and/or pure or doped single-crystal salts of these metals (principally thorium, uranium, neptunium, and plutonium).[1] This body of work has been key to developing theoretical frameworks for evaluating such effects as spin−orbit

* To whom correspondence should be addressed. E-mail: demorris@lanl.gov (D.E.M.); kiplinger@lanl.gov (J.L.K.).

10.1021/om049634v CCC: $27.50
Publication on Web 09/22/2004

coupling, crystal-field interactions, and, to a lesser extent, the degree of interaction between metal and ligand orbitals in these complexes. The organometallic chemistry of these early-actinide metals is dominated by metallocene complexes, in particular those containing the cyclopentadienyl anion ($C_5H_5^-$) and its substituted variants such as the pentamethylcyclopentadienyl anion ($C_5Me_5^-$).[2,3] Organoactinide chemistry has provided substantial diversity in both the symmetry of the complexes and the steric and electronic properties of the ligand sets. For example, it has proven possible to synthesize, isolate, and structurally characterize complexes with a host of ancillary ligands capable of σ- and π-interactions with the metal and for a range of metal oxidation states from trivalent to hexavalent.[3−6] Complexes having these electronically rich and structurally diverse ancillary ligands are typically not accessible in classical aqueous coordination chemistry.

Because these actinide metallocene complexes possess such rich electronic and structural diversity, they provide an ideal platform to systematically explore the effects of molecular structure and metal−ligand bonding on electronic structure and redox energetics. Surprisingly, however, there have been relatively few reports related to either the electronic spectral behavior[7−9] or electrochemical properties[10−16] of these complexes, although a number of researchers have noted the importance of the redox chemistry in understanding the reactivity trends in these complexes.[11,12,16] Recent synthetic progress in our laboratory has extended the range of uranium and thorium organometallic complexes based on a $(C_5Me_5)_2An$ structural core (An = U(IV), Th(IV) principally, but including a few U(VI) examples),[17−20] enabling such systematic investigations. This series preserves the nominal 2-fold symmetry at the metal center imposed by the $(C_5Me_5)_2An$ structural core but spans a range of ancillary ligands in the wedge between the pentamethylcyclopentadienyl rings having varying degrees of σ- and/or π-donor character. Thus, in addition to the known and structurally well-characterized dihalide (e.g., $(C_5Me_5)_2AnCl_2$)[21] and bis(alkyl) (e.g., $(C_5Me_5)_2An(CH_3)_2$) complexes,[17,21] we now have available complexes containing the more electronically rich hydrazonato ($\eta^2(N,N')$-RNN=CPh$_2$)[18,22] and ketimido (−N=C(R)(R′)) ligands.[19,23]

In this report we present and summarize cyclic voltammetric data and UV−visible−near-IR electronic absorption spectroscopic data for a broad range of complexes based on the $(C_5Me_5)_2An$ structural unit and compare these results to existing published data on structurally analogous systems. These new results reveal trends in oxidation-state (de)stabilization based on the electronic properties of the ancillary ligands. The spectral data obtained for these complexes also clearly reveal variations in the electronic structural properties that are linked to the extent of interaction between the ligand orbitals and the metal-based 5f and 6d orbitals. While no attempt has been made to rigorously interpret the detailed f−f electronic spectral data and make assignments of states derived from the $5f^2$ configuration, we provide a qualitative interpretation for the principal features of these data within the context of hypersensitivity and covalency in the metal−ligand bonding interactions. In total, these electrochemical and spectroscopic data provide important new insights into the role of the ancillary ligands in tuning electronic and steric properties and metal−ligand interactions.

Results and Discussion

Summary of Complexes and Structures. A compilation of all the uranium and thorium pentamethylcyclopentadienyl complexes that have been investigated as part of this study is provided in Figure 1. All complexes were prepared and characterized as described elsewhere (see Experimental Section). Most of these are bent metallocenes having pseudotetrahedral metal coordination geometry from the four ligand groups and approximate 2-fold symmetry at the metal center. The exceptions are the complexes (pentamethylcyclopentadienyl)tribenzyluranium(IV) (**3**; pseudotetrahedral but with ∼3-fold symmetry) and bis(pentamethylcyclopentadienyl)imidouranium(IV) (**13**; 2-fold symmetry, but not with pseudotetrahedral geometry).

Redox Properties from Cyclic Voltammetric Studies. Although there have been relatively few reports on the redox behavior of organoactinide complexes, particularly those of $C_5H_5^-$ or $C_5Me_5^-$ ligands,[10−16] these complexes do appear to be generally well-behaved toward redox processes at Pt or graphite electrodes in aprotic solvents such as THF that are themselves relatively poor ligands. We *have* observed that the choice of supporting electrolyte for these studies is critical for two reasons. First, common electrolytes used in non-

(1) Katz, J. J., Seaborg, G. T., Morss, L. R., Eds. *The Chemistry of the Actinide Elements*, 2nd ed.; Chapman and Hall: New York, 1986.
(2) Bursten, B. E.; Strittmatter, R. J. *Angew. Chem., Int. Ed. Engl.* **1991**, *30*, 1069−1085.
(3) Marks, T. J., Fragala, I. L., Eds. *Fundamental and Technological Aspects of Organo-f-Element Chemistry*; D. Reidel: Dordrecht, Holland, 1985.
(4) Marks, T. J. *Prog. Inorg. Chem.* **1979**, *25*, 223−333.
(5) Marks, T. J. *Science* **1982**, *217*, 989−997.
(6) Marks, T. J.; Ernst, R. D. In *Comprehensive Organometallic Chemistry*; Wilkinson, G., Stone, F. G. A., Abel, E. W., Eds.; Pergamon Press: Oxford, U.K., 1982; Chapter 21.
(7) Arnaudet, L.; Folcher, G.; Marquetellis, H.; Klahne, E.; Yunlu, K.; Fischer, R. D. *Organometallics* **1983**, *2*, 344−346.
(8) Marquet-Ellis, H.; Folcher, G. *J. Organomet. Chem.* **1977**, *131*, 257−261.
(9) Zanella, P.; Brianese, N.; Casellato, U.; Ossola, F.; Porchia, M.; Rossetto, G.; Graziani, R. *Inorg. Chim. Acta* **1988**, *144*, 129−134.
(10) Clappe, C.; Leveugle, D.; Hauchard, D.; Durand, G. *J. Electroanal. Chem.* **1998**, *448*, 95−103.
(11) Hauchard, D.; Cassir, M.; Chivot, J.; Ephritikhine, M. *J. Electroanal. Chem.* **1991**, *313*, 227−241.
(12) Hauchard, D.; Cassir, M.; Chivot, J.; Baudry, D.; Ephritikhine, M. *J. Electroanal. Chem.* **1993**, *347*, 399−407.
(13) Schnabel, R.; Scott, B.; Smith, W.; Burns, C. *J. Organomet. Chem.* **1999**, *591*, 14−23.
(14) Sonnenberger, D. C.; Gaudiello, J. G. *Inorg. Chem.* **1988**, *27*, 2747−2748.
(15) Ossola, F.; Zanella, P.; Ugo, P.; Seeber, R. *Inorg. Chim. Acta* **1988**, *147*, 123−126.
(16) Finke, R. G.; Gaughan, G.; Voegeli, R. *J. Organomet. Chem.* **1982**, *229*, 179−184.
(17) Kiplinger, J. L.; Morris, D. E.; Scott, B. L.; Burns, C. J. *Organometallics* **2002**, *21*, 5978−5982.
(18) Kiplinger, J. L.; John, K. D.; Morris, D. E.; Scott, B. L.; Burns, C. J. *Organometallics* **2002**, *21*, 4306−4308.
(19) Kiplinger, J. L.; Morris, D. E.; Scott, B. L.; Burns, C. J. *Organometallics* **2002**, *21*, 3073−3075.
(20) Kiplinger, J. L.; Morris, D. E.; Scott, B. L.; Burns, C. J. *Chem. Commun.* **2002**, 30−31.
(21) Fagan, P. J.; Manriquez, J. M.; Maatta, E. A.; Seyam, A. M.; Marks, T. J. *J. Am. Chem. Soc.* **1981**, *103*, 6650−6667.
(22) Kiplinger, J. L.; Jantunen, K. C.; Scott, B. L.; Hay, P. J.; Morris, D. E.; Burns, C. J. Manuscript in preparation.
(23) Jantunen, K. C.; Castro-Rodriguez, I.; Da Re, R. E.; Golden, J. T.; Taw, F. L.; Morris, D. E.; Scott, B. L.; Burns, C. J.; Kiplinger, J. L. *Organometallics* **2004**, *23*, 4682−4692.

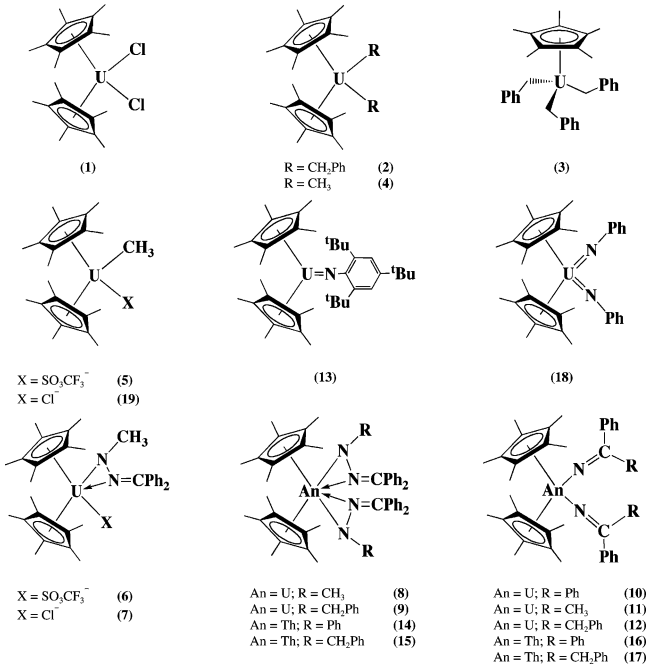

Figure 1. Pentamethylcyclopentadienyl actinide complexes.

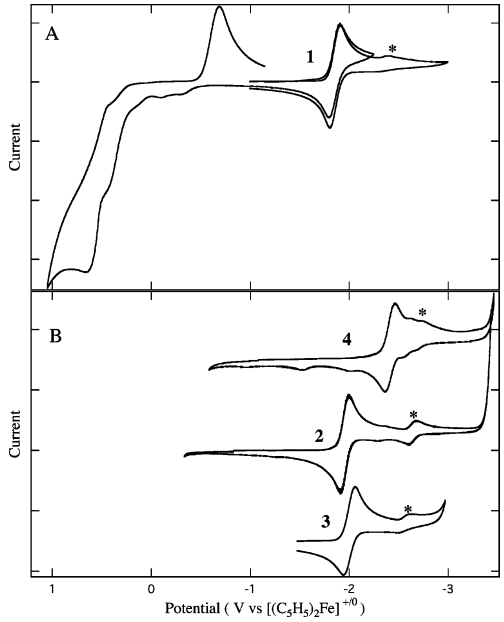

Figure 2. Cyclic voltammetric data for $(C_5Me_5)_2U^{IV}$ complexes possessing σ-donor ligands obtained in ~0.1 M [(n-$C_4H_9)_4N$][$B(C_6F_5)_4$]/THF at 200 mV/s: $(C_5Me_5)_2UCl_2$ (**1**); $(C_5Me_5)_2U(CH_2Ph)_2$ (**2**); $(C_5Me_5)U(CH_2Ph)_3$ (**3**); $(C_5Me_5)_2U(CH_3)_2$ (**4**). Asterisks denote waves attributed to minor ligand redistribution products. See text for discussion.

aqueous solvents such as quaternary ammonium hexafluorophosphate or tetrafluoroborate present problems presumably because of the fluorophilic nature of the actinides. Initial efforts to obtain voltammetric data in THF solutions of these electrolytes showed indications of slow sample decomposition, likely from fluoride abstraction chemistry from the electrolyte anions. Similar behavior has been reported in other electrochemical studies of organouranium complexes.[16,24] Second, although these electrolytes have reasonable solubility in very low dielectric solvents such as THF, the solution resistance remains quite high (10−100 kΩ/cm is not uncommon in our cell), so that even with electronic compensation for the resistance, the waves from the Faradaic processes can become masked and/or unacceptably distorted. We have overcome both of these experimental problems through the use of [(n-$C_4H_9)_4N$]-[$B(C_6F_5)_4$] as the electrolyte. The advantageous properties of this quarternary ammonium salt as an electrolyte for voltammetric studies in low dielectric constant solvents have been noted in several recent reports,[25,26] and the origin of this advantageous effect has recently been demonstrated to be directly related to the greater dissociation of the cation/anion pair in low dielectric media such as THF as a result of the more highly delocalized charge in the $[B(C_6F_5)_4]^-$ anion.[27] Furthermore, this anion appears to be inert toward fluoride abstraction chemistry.

Using this combination of Pt or graphite working electrode, THF solvent, and [(n-$C_4H_9)_4N$][$B(C_6F_5)_4$] electrolyte, we have been successful in obtaining cyclic voltammetric data for the entire range of complexes under investigation in this report. Our focus is on the redox waves attributable to the uranium-metal-based processes to investigate the influence of the ancillary ligands on the energetics of the metal-based redox couples. In particular, we have observed one or more electrochemically reversible metal-based redox waves for all of the uranium complexes. Additional voltammetric waves are also observed for many of the uranium complexes, which are ascribed to processes localized on the ancillary ligands. Not surprisingly, for the tetravalent complexes $(C_5Me_5)_2Th$ (**14**−**17**) we did not observe any metal-based redox waves, since these all have nominally $6d^05f^0$ ground electronic states and these metal valence orbitals are typically outside the accessible potential window of all common solvent/electrolyte systems.[16] However, as discussed below in greater detail, the voltammetric data for these thorium organometallics have been critical in distinguishing between metal- and ligand-based electrochemical processes in the isostructural uranium complexes. Finally, all complexes studied exhibit irreversible oxidative voltammetric processes (Figure 2A) at potentials positive of ~+0.5 V vs $[(C_5H_5)_2Fe]^{+/0}$. Similar processes have been observed in cyclopentadienyl and pentamethylcyclopentadienyl complexes of lanthanides (e.g., $(C_5Me_5)_2Yb(bpy)$)[28,29] and d^0 transition metals (e.g., $(C_5Me_5)_2ZrCl_2$)[30] and are ascribed to C_5H_5- or C_5Me_5-localized processes.

For all of the tetravalent uranium complexes studied here, the voltammetric behavior can be classified into one of only two categories, and these behaviors and the complexes they encompass will be used to organize the ensuing discussion. Category 1 includes the complexes

(24) Maury, O.; Ephritikhine, M.; Nierlich, M.; Lance, M.; Samuel, E. *Inorg. Chim. Acta* **1998**, *279*, 210−216.
(25) Camire, N.; Mueller-Westerhoff, U. T.; Geiger, W. E. *J. Organomet. Chem.* **2001**, *637*, 823−826.
(26) LeSuer, R. J.; Geiger, W. E. *Angew. Chem., Int. Ed.* **2000**, *39*, 248−250.
(27) LeSuer, R. J.; Buttolph, C.; Geiger, W. E. *Anal. Chem.*, in press.
(28) Kuehl, C.; Da Re, R.; Scott, B.; Morris, D.; John, K. *Chem. Commun.* **2003**, 2336−2337.
(29) Da Re, R.; Kuehl, C.; Brown, M.; Rocha, R.; Bauer, E.; John, K.; Morris, D.; Shreve, A.; Sarrao, J. *Inorg. Chem.* **2003**, *42*, 5551−5559.
(30) Strittmatter, R. J.; Morris, D. E.; Bursten, B. E. Unpublished results, 2004.

Table 1. Summary of Voltammetric Data for $(C_5Me_5)_2An$ Systems

	metal-based wave			
	$E_{1/2}$ (V vs $[C_5H_5]_2Fe^{+/0}$)		ΔE (V)	ligand-based wave
complex[a]	An(IV)/An(III)	An(V)/An(IV)	((V/IV) − (IV/III))	$E_{1/2}$ (V vs $[C_5H_5]_2Fe^{+/0}$)
	An = U(IV), Category 1			
1	−1.85			
2	−1.95 (−2.64)[b]			
3	−2.00			
4	−2.41			
5	−1.83 (−1.32, −2.58)[b]			
	An = U(IV), Category 2			
6	−2.01	0.18	2.19	
7	−2.29 (−1.81)[b]	−0.07	2.22	
10	−2.50	−0.48	2.02	−2.79
9	−2.56	−0.47	2.09	−3.0[c]
12	−2.57	−0.46	2.11	
13	−2.61	−0.73	1.88	−2.9 (−0.25, 0.48)[d]
11	−2.68	−0.54	2.14	−2.96
8	−2.78	−0.68	2.10	-3.1[c]
	An = Th(IV)			
14				−3.0[c]
15				−3.1[c]
16				−2.8[c]
17				−2.9,[c] −3.0[c]
	An = U(VI)			
18	−1.70[e]	−2.00[f]		−2.8[c]

[a] See Figure 1 for identification of complexes. [b] Lower current wave attributed to ligand redistribution product(s), see text. [c] Irreversible wave. [d] Ligand oxidation waves. [e] U(VI)/U(V) [f] U(V)/U(IV); This assignment is tentative.

$(C_5Me_5)_2UCl_2$ (**1**), $(C_5Me_5)_2UR_2$ (R = CH_2Ph (**2**), CH_3 (**4**)), $(C_5Me_5)U(CH_2Ph)_3$ (**3**), and $(C_5Me_5)_2U(CH_3)(SO_3CF_3)$ (**5**). Category 2 includes the hydrazonato complexes $(C_5Me_5)_2U(X)(\eta^2(N,N')$-$CH_3NN{=}CPh_2)$ (X = $SO_3CF_3^-$ (**6**), Cl^- (**7**)), $(C_5Me_5)_2U(\eta^2(N,N')$-$CH_3NN{=}CPh_2)_2$ (**8**), and $(C_5Me_5)_2U(\eta^2(N,N')$-$CH_2PhNN{=}CPh_2)_2$ (**9**), the ketimido complexes $(C_5Me_5)_2U[-N{=}C(Ph)(R)]_2$ (R = Ph (**10**), CH_3 (**11**), CH_2Ph (**12**)), and the imido complex $(C_5Me_5)_2U{=}N$-2,4,6-$^tBu_3C_6H_2$ (**13**). Note that all category 2 complexes possess at least one nitrogen-donor ligand. Finally, for comparison we include data for some Th hydrazonato (**14**, **15**) and ketimido (**16**, **17**) complexes that are structurally analogous to the uranium complexes in category 2 and the hexavalent uranium bis(imido) complex $(C_5Me_5)_2U(=NPh)_2$ (**18**). A complete list of redox potentials for all complexes is provided in Table 1.

Category 1 Complexes. The ancillary ligands in the first category of complexes are all principally σ-donors, and the voltammetry in this category is dominated by a single metal-based reduction process, U(IV)/U(III), that occurs between ∼−1.8 and −2.6 V vs $[(C_5H_5)_2Fe]^{+/0}$, as illustrated in Figure 2. If the potential range of the voltammetric scan encompasses only the U(IV)/U(III) reduction process, this voltammetric wave for all complexes in this category is characterized according to the standard criteria to be a reversible one-electron process, but with varying degrees of influence from sluggish electron-transfer kinetics, as noted by the change in the potential separation between cathodic and anodic peaks with increasing scan rate.[31] Excursions to very negative potential values (near the solvent window limit) or into the region of the proposed C_5Me_5-based redox processes result in distortions to one or both cathodic and anodic peak components in the U(IV)/U(III) wave, indicative of coupled chemical reactions associated with these other electron-transfer steps that alter the structure of the complex. Finally, for several of these complexes, there are additional, lower peak current voltammetric waves (indicated by asterisks in Figure 2) that are attributed to metal-based couples for new species formed by ligand displacement and/or redistribution processes. These reactions are described further below.

Our results for this class of compounds are in generally good agreement with those obtained previously for $(C_5Me_5)_2UCl_2$[14,16] and other related systems.[10−12,15] In particular, in previous cyclic voltammetric studies, the U(IV)/U(III) redox couple has been found to be reversible to quasi-reversible for $(C_5Me_5)_2UCl_2$, $(C_5H_5)_2U(BH_4)_2$, and a host of tris(C_5H_5) and tris(C_5H_4R) complexes, including $(C_5H_5)_3UCl$, $(C_5H_5)_3U(BH_4)$, and $(C_5H_4R)_3UCl$ (R = H, CH_3, $(CH_3)_3C$, $(CH_3)_3Si$). Although meaningful comparisons between the voltammetric data reported in these studies are complicated by the fact that different supporting electrolytes and reference electrode/cell geometries were employed, we estimate that the potential for the U(IV)/U(III) couple lies between ∼−1.5 V and −2.2 V vs $[(C_5H_5)_2Fe]^{+/0}$ in all studies. A more useful comparison is the variability in the U(IV)/U(III) redox potential with ligand environment within the comparative studies of differing ligand sets. For example, Sonnenberger et al. found that the U metal center became more difficult to reduce in the series $(C_5H_5)_3UCl < (C_5H_5)_4U < (C_5Me_5)_2UCl_2$.[14] This corresponds to the stabilization of the tetravalent oxidation state from the electron-donating ability of the ligands with $C_5Me_5^- > C_5H_5^- > Cl^-$. Similarly, Hauchard et al. showed that the reduction potential for the borohydride complexes reflects the greater donor character of $C_5H_5^-$ versus BH_4^- such that $(C_5H_5)_3U(BH_4)$ was more difficult to reduce than $(C_5H_5)_2U(BH_4)_2$.[12] In a related study, Clappe et al. reported that the U(IV) metal center in $(C_5H_4R)_3UCl$ complexes becomes more difficult to reduce across the series R = $(CH_3)_3Si < H < (CH_3)_3C < CH_3$.[10] Again, this trend correlates roughly with the electron-donating ability of the $C_5H_4R^-$ ligand, except, as the authors note, for the apparent reversal of the methyl- and *tert*-butyl-substituted $C_5H_5^-$ ligands. The trend in the reduction potential of the U(IV) metal center in the category 1 complexes studied here is provided in Table 1. Clearly for the category 1 members, the reduction potentials reflect the more strongly electron-donating nature of the alkyl groups relative to chloride ion, with the methyl group much more so than the benzyl group.

None of the complexes in the first category in this investigation show any distinct evidence for a metal-based U(V)/U(IV) oxidation process. However, for a few of the tris(cyclopentadienyl) complexes considered in these previous studies, there was evidence in the voltammetry for a U(V)/U(IV) redox couple. The existence of this redox process appears to correlate strongly with substantial electron density around the metal center found in the tris(cyclopentadienyl) systems. Thus, a U(V)/U(IV) wave is reported for $(C_5H_5)_3U(NEt_2)$,[15] $(C_5H_5)_3UCl$,[10] and all of the $(C_5H_4R)_3UCl$ complexes.[10]

(31) Bard, A. J.; Faulkner, L. R. *Electrochemical Methods: Fundamentals and Applications*, 2nd ed.; Wiley: New York, 2001.

However, in all instances except for the mono(amide) complex, the U(V)/U(IV) couple is proposed to be linked to a following chemical reaction that degrades the voltammetric behavior. The chemical process is suggested to be a disproportionation reaction of the U(V) species, in part on the basis of the commonly observed instability of this uranium oxidation state. However, as discussed below for the complexes in the second category studied here, the U(V) state is stable for many systems, at least on a voltammetric time scale.

As noted above, additional lower peak-current reduction waves are observed in the cyclic voltammograms of most of the complexes (**1**−**4**) in category 1 (waves indicated with asterisks in Figure 2). For complex **5**, $(C_5Me_5)_2U(CH_3)(SO_3CF_3)$, two reversible reduction waves of approximately equal peak current are observed. These additional voltammetric reduction waves are present immediately upon dissolution of the complexes in THF/electrolyte solution, and the peak current remains constant relative to that of the principal U(IV)/U(III) wave for the parent complex throughout the course of the voltammetric experiment. Thus, these waves do NOT arise from coupled chemical processes linked to the redox processes of the parent complex but instead appear to reflect a small equilibrium concentration of a secondary electroactive species. Similar observations have been made in the previous electrochemical study of $(C_5H_5)_2U(BH_4)_2$, and the behavior was attributed to a ligand exchange reaction to give $(C_5H_5)U(BH_4)_3$ and $(C_5H_5)_3U(BH_4)$.[12] The authors suggest that this process is promoted by the high ionic strength from the electrolyte in the electrochemical solution. Ligand exchange reactions have also been reported for $(C_5H_5)_2UCl_2$ in neat THF solution to give mono- and tris(cyclopentadienyl) complexes.[32] Simple ligand redistribution reactions such as this could easily give rise to more than two different electroactive species in the electrochemical solution. We observe only two electrochemically resolved species in most of the systems reported here (the "parent" and one additional species). Thus, it is not clear if the chemistry in our systems is similar to that of the ligand-exchange reactions reported previously. However, NMR data on the parent complexes in toluene show no evidence for secondary species (e.g., from impurities or ligand redistribution). Thus, either the electrolyte or the THF solvent (or both) is implicated in promoting the formation of the additional electroactive species observed in our electrochemical studies. Additional studies of this phenomenon are underway.

Category 2 Complexes. All of the complexes in this category contain one or two nitrogen-containing ligands that have the capability to interact with the metal center in both σ- and π-modes via the nitrogen lone pair orbitals and/or the π-orbital system on the ligand. As with the complexes in category 1, all these category 2 complexes (**6**−**13**) exhibit a reversible reduction wave at potentials between ∼−2 and −2.8 V vs $[(C_5H_5)_2Fe]^{+/0}$ that is attributable to a metal-based U(IV)/U(III) process. Typical examples are provided in Figure 3A,B. Here, too, the voltammetric characteristics of this reduction wave are consistent with a simple, reversible one-electron process. The distinguishing feature of the category 2 complexes (relative to those in category 1) is the appearance of an oxidative voltammetric process in the potential region from ∼+0.2 to −0.7 V vs $[(C_5H_5)_2Fe]^{+/0}$. This wave also has the voltammetric characteristics of a simple, reversible one-electron process and is attributed to the metal-based U(V)/U(IV) redox couple. Unlike the behavior previously reported for other electron-rich U(IV) tris(cyclopentadienyl) complexes, for the complexes of these nitrogen-containing ligands the U(V) species appears to be stable on a voltammetric time scale with no evidence for coupled chemical reactivity such as disproportionation.

The influence of these nitrogen-based ligands on the redox energetics in these tetravalent $(C_5Me_5)_2U$ complexes is particularly noteworthy in comparison to the redox energetics in the category 1 complexes and most other cyclopentadienyl complexes of tetravalent uranium. In most of the cases investigated here it was found that the nitrogen-containing ligands provide the same measure of stabilization of tetravalent uranium as the alkyl ligands in the bis- and tris(alkyl) complexes. Thus, the potential of the U(IV)/U(III) couple is shifted to quite negative potentials compared to that of, for example, the dihalide complex. However, in the case of the nitrogen-containing ligands (including the amido ligand in $(C_5H_5)_3U(NEt_2)$),[15] the metal center becomes so electron rich that the one-electron-oxidation process is readily accessible and yields a stable pentavalent complex. While the pentavalent oxidation state of uranium is noted for its instability toward disproportionation in aqueous environments (where it typically exists as the trans dioxo cation generated from the hexavalent precursor, UO_2^{2+}), it has been demonstrated to be stable on a voltammetric time scale for some ligand environments.[33] The difference between these category 2 complexes and those in category 1 is the ability of the nitrogen ligands to engage in π-bonding with the metal center. Undoubtedly, in these $(C_5Me_5)_2U$ complexes possessing ketimido (−N=C(R)(R′)) or hydrazonato (η^2-(*N*,*N*′)-RNN=CPh$_2$) ligands, the stability of the pentavalent oxidation state derives from the additional π interaction between these nitrogen ligands and the metal center, stabilizing the high-valent oxidation state in a way that simple σ-donor ligands alone cannot. This π-bonding interaction has been substantiated in recent density functional theory calculations.[22]

The category 2 complexes do not appear to be as susceptible to ligand exchange chemistry as those in category 1. Thus, the additional lower current voltammetric peaks indicative of these equilibrium products in the electrochemical solutions are relatively rare in this category of complexes. In contrast, however, because the nitrogen ligands in the category 2 complexes possess accessible nonbonding-p, π, and π* orbitals of energies comparable to those of the valence metal 5f orbitals, many of these complexes do present additional voltam-
metric features derived from ligand-localized redox processes. These are principally irreversible reduction waves that occur at potentials more negative than the U(IV)/U(III) couples in the ketimido and hydrazonato complexes, as illustrated in Figure 3. The assignment

(32) Bagnall, K. W.; Edwards, J.; Tempest, A. C. *J. Chem. Soc., Dalton Trans.* **1978**, 295−298.

(33) Morris, D. E. *Inorg. Chem.* **2002**, *41*, 3542−3547.

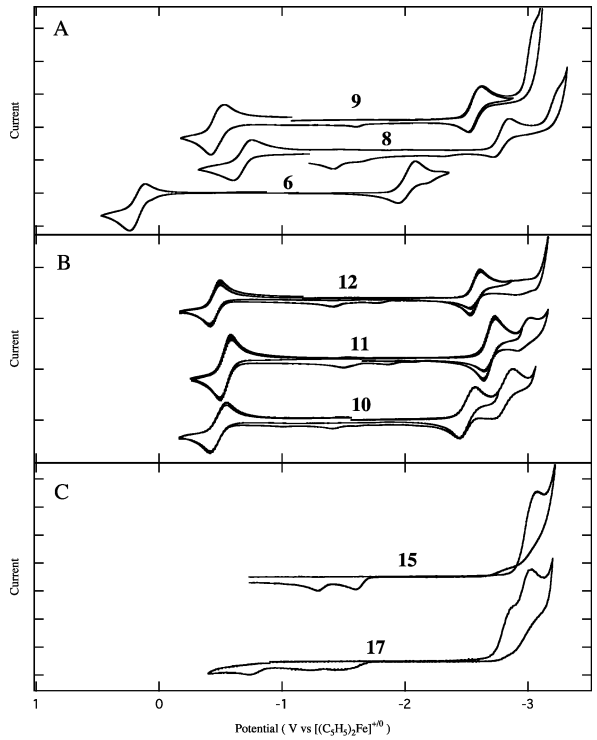

Figure 3. Cyclic voltammetric data for $(C_5Me_5)_2An^{IV}$ complexes possessing nitrogen donor ligands obtained in ~0.1 M $[(n\text{-}C_4H_9)_4N][B(C_6F_5)_4]$/THF at 200 mV/s: (A) U(IV) hydrazonato complexes $(C_5Me_5)_2U(\eta^2(N,N')\text{-}CH_3NN{=}CPh_2)(SO_3CF_3)$ (**6**), $(C_5Me_5)_2U[\eta^2(N,N')\text{-}CH_3NN{=}CPh_2]_2$ (**8**), and $(C_5Me_5)_2U[\eta^2(N,N')\text{-}CH_2PhNN{=}CPh_2]_2$ (**9**); (B) U(IV) ketimido complexes $(C_5Me_5)_2U[-N{=}C(Ph)_2]_2$ (**10**), $(C_5Me_5)_2U[-N{=}C(Ph)(CH_3)]_2$ (**11**), and $(C_5Me_5)_2U[-N{=}C(Ph)(CH_2Ph)]_2$ (**12**); (C) $(C_5Me_5)_2Th^{IV}$ hydrazonato and ketimido complexes $(C_5Me_5)_2Th[\eta^2(N,N')\text{-}CH_2PhNN{=}CPh_2]_2$ (**15**) and $(C_5Me_5)_2Th[-N{=}C(Ph)(CH_2Ph)]_2$ (**17**).

of these waves to ligand-based processes is confirmed on the basis of comparison to the structurally analogous $(C_5Me_5)_2Th$ complexes (Figure 3C), for which no metal-based redox chemistry is expected. Note that the reductive redox processes in these thorium complexes appear at potentials nearly identical to those of the analogous uranium complexes. The irreversibility in these reductive ligand redox processes suggests that there are chemical reactions coupled to these electron-transfer steps. Indeed, if the potential scans proceed into these ligand-based reduction waves, the metal-based redox waves for the uranium complexes become degraded and new oxidative peaks are observed at ~−1.5 V vs $[(C_5H_5)_2Fe]^{+/0}$ for both the uranium and thorium complexes. The nature of the ligand-based chemical transformations following the reduction step is unknown. The $(C_5Me_5)_2U$ imido complex (**13**) is unique in this series of complexes, in that it possesses two additional oxidation waves at potential values slightly positive of the U(V)/U(IV) oxidation wave. The proximity of these waves to the U(V)/U(IV) oxidation wave renders an assignment of either of these waves to a metal-based U(VI)/U(V) couple unlikely and suggests that they are most likely attributable to ligand-based oxidation processes. Both of these putative ligand-based oxidation steps possess both anodic and cathodic voltammetric peaks consistent with a chemically reversible electron-transfer step (i.e., no chemical degradation accompanies the electron transfer), and neither leads to any significant distortion of the U(V)/U(IV) wave. Thus, the imido complex appears to remain intact on a voltammetric time scale following the removal of two additional electrons from ligand-based orbitals.

Hexavalent Uranium Complexes. The electrochemical behavior of the hexavalent uranium complex **18** provides an interesting contrast to that for the U(IV) complexes. This complex shows a single electrochemically reversible couple at ~−1.7 V vs $[(C_5H_5)_2Fe]^{+/0}$ as the dominant feature in the voltammetry. This wave is assigned to the U(VI)/U(V) transformation. It is rather remarkable that this potential is nearly as negative as the U(IV)/U(III) couple in the category 1 and 2 complexes (Table 1). This clearly demonstrates how important the electron-donating ability of the ligands (in this case to form a metal−ligand multiple bond) is in stabilizing the metal oxidation state. This complex also possesses additional irreversible reduction waves at potentials negative of the assigned U(VI)/U(V) wave. The wave at −2.00 V has been tentatively assigned to a metal-based U(V)/U(IV) process, although the potential separation between this wave and that attributed to the U(VI)/U(V) couple is rather small for a second metal-based reduction step.

Additional Comparisons from Redox Properties. One of the more interesting trends identified in this investigation relating to the redox energetics is that in the category 2 complexes the potential separation between the U(V)/U(IV) couple and the U(IV)/U(III) couple remains nearly constant over the entire series of complexes (Table 1). The average value for this separation for the eight complexes is 2.09 ± 0.04 V. As noted above, several of the published voltammetric studies of U(IV) metallocene complexes report both U(V)/U(IV) and U(IV)/U(III) couples. For $(C_5H_5)_3U(NEt_2)$, which is reported to have a reversible U(V)/U(IV) couple, the potential separation between the oxidation and reduction couples is 2.10 V.[15] For the other complexes, the oxidation couple is reportedly tied to a following chemical reaction that may make determination of the true half-wave potential for the U(V)/U(IV) couple difficult. Nonetheless, the potential separation between these couples for $(C_5H_5)_3UCl$ and $(C_5H_4Me)_3UCl$ is 2.10 and 2.05 V, respectively.[10] Thus, it appears that this potential separation is consistent across most U(IV) cyclopentadienyl complexes having high electron density at the metal center.

In contrast, the potential separation between the metal-based reduction and oxidation processes for other U(IV) metallocene systems having lesser degrees of electron density at the metal center (i.e., category 1 complexes and other bis(cyclopentadienyl) complexes whose electrochemistry has been reported) must be substantially greater than this ~2.1 V value. For the category 1 systems, the U(V)/U(IV) couple was not identified in our investigations. We cannot rule out the possibility that the voltammetric wave for this process is overlapping with the proposed C_5Me_5-based oxidation process. This latter process has very broad, ill-defined wave(s) associated with it (Figure 2A), making discernment of a potential underlying discrete metal-based oxidation process difficult. However, if we assume that a metal-based U(V)/U(IV) couple is buried within this

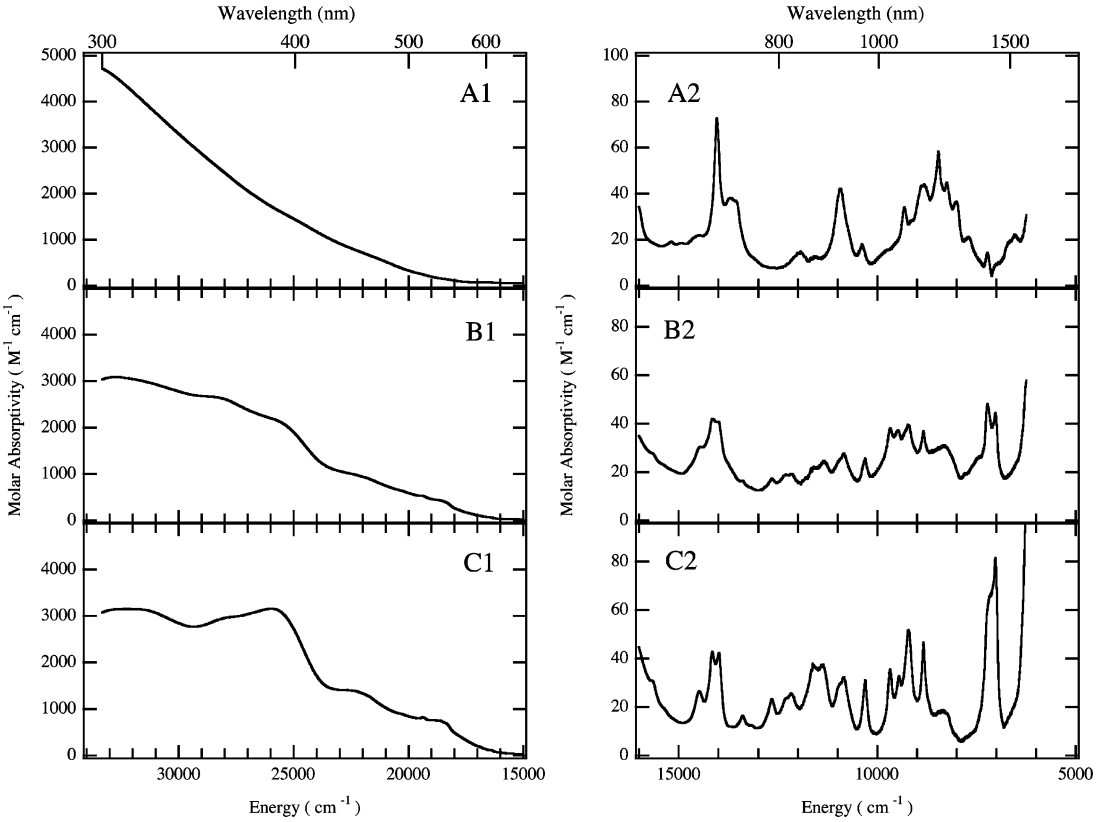

Figure 4. UV−visible−near-infrared electronic absorption spectra for toluene solutions of $(C_5Me_5)_2U^{IV}$ complexes possessing σ-donor ligands: (A1 and A2) $(C_5Me_5)_2U(CH_3)_2$ (**4**); (B1 and B2) $(C_5Me_5)_2U(CH_3)(Cl)$ (**19**); (C1 and C2) $(C_5Me_5)_2UCl_2$ (**1**).

complicated oxidation response at ∼0.5−1.0 V, we can establish a minimum separation between the U(V)/U(IV) and U(IV)/U(III) couples for these category 1 complexes of at least 2.8 V (for $(C_5Me_5)_2UCl_2$, which has the most positive metal-based reduction wave). Thus, the high electron density found in the category 2 and tris(cyclopentadienyl) complexes provides, at a minimum, ∼0.7 V of added stabilization to the pentavalent metal center.

Electronic Structure and Properties from Optical Spectroscopy. The UV−visible−near-infrared electronic absorption spectra for these $(C_5Me_5)_2U^{IV}$ complexes all have two different energy regions of interest. Typical spectra obtained for toluene solutions of these complexes are shown in Figures 4−6. The first region, which lies below ∼15 000 cm^{-1}, contains bands attributable to electronic transitions between the states derived from the $5f^2$ electronic configuration. Note that this region is limited on the low-energy (long wavelength) end by solvent vibrational overtone absorptions that preclude obtaining meaningful absorbance data for the complexes below ∼6000 cm^{-1}. The second region lies at energies above ∼15 000 cm^{-1}. This region is limited on the high-energy (short wavelength) end at ∼32 000 cm^{-1} by electronic transitions within the solvent itself. Assignment of the broad, less structured, but more intense bands in this region is less straightforward, because there are many different electronic states potentially present in these complexes. For the most part, this region will contain transitions derived from promotion of a 5f electron into higher lying metal-based 6d orbitals as well as charge-transfer transitions involving the ligand-based orbitals. These latter transitions, in particular, figure prominently in the ensuing discussion. Finally, note that the $(C_5Me_5)_2U$ structural core remains constant throughout these complexes, with the exception of the tris(benzyl) complex (**3**). Thus, two very important molecular structural features that establish a baseline for the f−f electronic structure, the symmetry at the metal center and the crystal field induced by the bis(pentamethylcyclopentadienyl) ligand framework, remain constant over nearly every complex (Figure 1). Thus, the focus in interpreting the spectral data can be placed on the role of the ancillary ligands, L_1 and L_2.

As with the voltammetric data discussed above, these electronic spectral data also fall into distinct classes related to the nature of the ancillary ligands bound to the $(C_5Me_5)_2U$ core. The first class of uranium(IV) complexes (**1**−**5**, **19**) in the electronic spectral comparison includes those that have ancillary ligands of essentially σ-donor character. Example spectra from this class are provided in Figure 4. All of the complexes in this class have a large number of narrow bands in the f−f region, and the numbers and energies of these bands are quite similar. The most important distinguishing characteristics of the spectra for this class of complexes are the low intensities of the f−f bands (molar absorptivity, ϵ, values of 10−80 M^{-1} cm^{-1}) and the presence of less well-resolved higher energy bands associated with f−d and charge-transfer transitions ($\epsilon \approx$ 2000−3000 M^{-1} cm^{-1}). The intensities in these f−f bands are similar to those seen in many classical coordination compounds of tetravalent uranium and other $5f^2$ actinide species,[34] as well as some tetrahedral U(IV) aryloxide complexes.[35−37] These intensities reflect the

(34) Carnall, W. T.; Crosswhite, H. M. In *The Chemistry of the Actinide Elements*, 2nd ed.; Katz, J. J., Seaborg, G. T., Morss, L. R., Eds.; Chapman and Hall: New York, 1986; Vol. 2, pp 1235−1277.

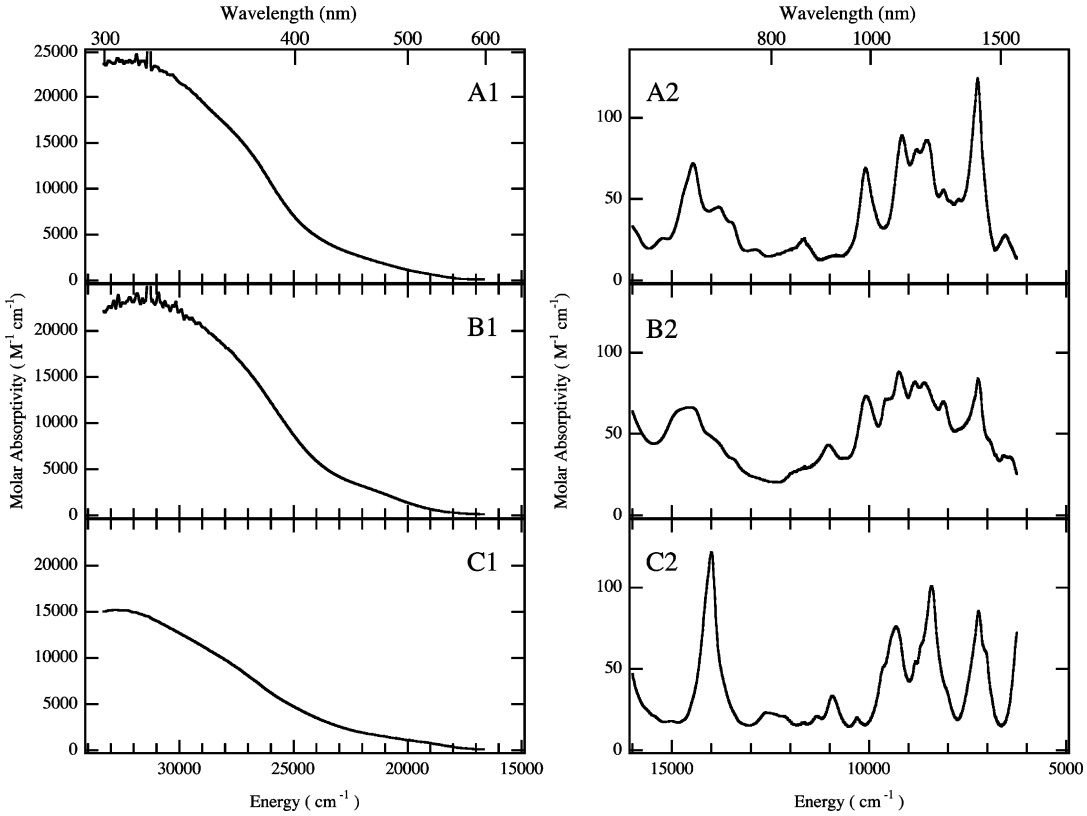

Figure 5. UV−visible−near-infrared electronic absorption spectra for toluene solutions of $(C_5Me_5)_2U^{IV}$ complexes possessing hydrazonato ligands: (A1 and A2) $(C_5Me_5)_2U[\eta^2(N,N')\text{-}CH_2Ph{-}N{-}N{=}CPh_2]_2$ (**9**); (B1 and B2) $(C_5Me_5)_2U[\eta^2(N,N')\text{-}CH_3{-}N{-}N{=}CPh_2]_2$ (**8**); (C1 and C2) $(C_5Me_5)_2U(\eta^2(N,N')\text{-}CH_3{-}N{-}N{=}CPh_2)(Cl)$ (**7**).

nominally Laporte parity forbidden character of these interconfiguration transitions,[34,38] even though these complexes lack rigorous inversion symmetry at the metal center. Note that these intensities are greater than those in most 4f complexes, as a result of the greater radial extent of the 5f orbitals and therefore the greater metal−ligand interactions found in 5f versus 4f complexes.[34] The transition intensities found in the higher energy spectral region for this class of complexes (Figure 4A1−C1) serve principally as a baseline for subsequent comparisons. The transitions in this region for this class will include metal-localized 5f−6d bands as well as charge-transfer transitions involving the $C_5Me_5^-$ and Cl^- ligands. The energies and intensities of these f−d and C_5Me_5-based charge-transfer transitions should remain fairly constant across the entire series of organouranium complexes reported here.

The second class of uranium(IV) complexes (**6**−**9**) from the optical spectroscopy perspective are those that contain a hydrazonato ligand. Typical spectra from this class are illustrated in Figure 5. As observed for the first class, complexes in this class also exhibit a high degree of correlation with respect to the number and relative energies of the bands in both the f−f and higher-energy regions of the spectrum. For spectra in this class, however, the intensity of the bands in the f−f region ($\epsilon \approx 30{-}120\ M^{-1}\ cm^{-1}$) is on average about 50% greater than for those in the first class discussed above. Moreover, the intensities of the broad bands in the higher energy region are increased dramatically ($\epsilon \approx 15\,000{-}20\,000\ M^{-1}\ cm^{-1}$) for this class of complexes. Since it is anticipated that transitions localized on the $(C_5Me_5)_2U$ core will be only moderately affected by substitution at L_1 and L_2 (vide supra), this dramatic increase in the intensity must be attributed to new electronic transitions available with these hydrazonato ligands, including both ligand-localized $\pi{-}\pi^*$ transitions and $U{-}L_{1,2}$ charge-transfer transitions.

The final class of uranium(IV) complexes in the optical spectroscopy comparison includes the imido (**13**) and ketimido (**10**−**12**) complexes. Representative spectra for the imido (**13**) and diphenylketimido (**10**) complexes are shown in Figure 6. For spectra in this last class there is an apparent decrease in the number of f−f bands in the low-energy region, but the number and position of the bands are also about the same for both complexes. The apparent decrease in the number of f−f bands is in part an artifact due to the encroachment of the broad, higher energy bands well into the near-infrared region in these complexes. Thus, the higher energy f−f bands are obscured by the more intense molecular-transition bands. Note also that the portion of the molecular transition region between ~15 000 and 25 000 cm^{-1} becomes significantly more structured for these complexes, suggesting the presence of additional lower energy excited states that are most likely charge transfer in character. Again, the intensity of these bands is a key feature. The f−f bands for this class of complexes are more intense ($\epsilon \approx 50{-}400\ M^{-1}\ cm^{-1}$) than

(35) Berg, J. M.; Clark, D. L.; Huffman, J. C.; Morris, D. E.; Sattelberger, A. P.; Streib, W. E.; Van Der Sluys, W. G.; Watkin, J. G. *J. Am. Chem. Soc.* **1992**, *30*, 10811−10821.
(36) Berg, J. M.; Sattelberger, A. P.; Morris, D. E.; Van Der Sluys, W. G.; Fleig, P. *Inorg. Chem.* **1993**, *3*, 647−653.
(37) Berg, J. M. *J. Alloys Compd.* **1994**, *213*, 497−499.
(38) Lever, A. B. P. *Inorganic Electronic Spectroscopy*; Elsevier: Amsterdam, 1984; Vol. 33.

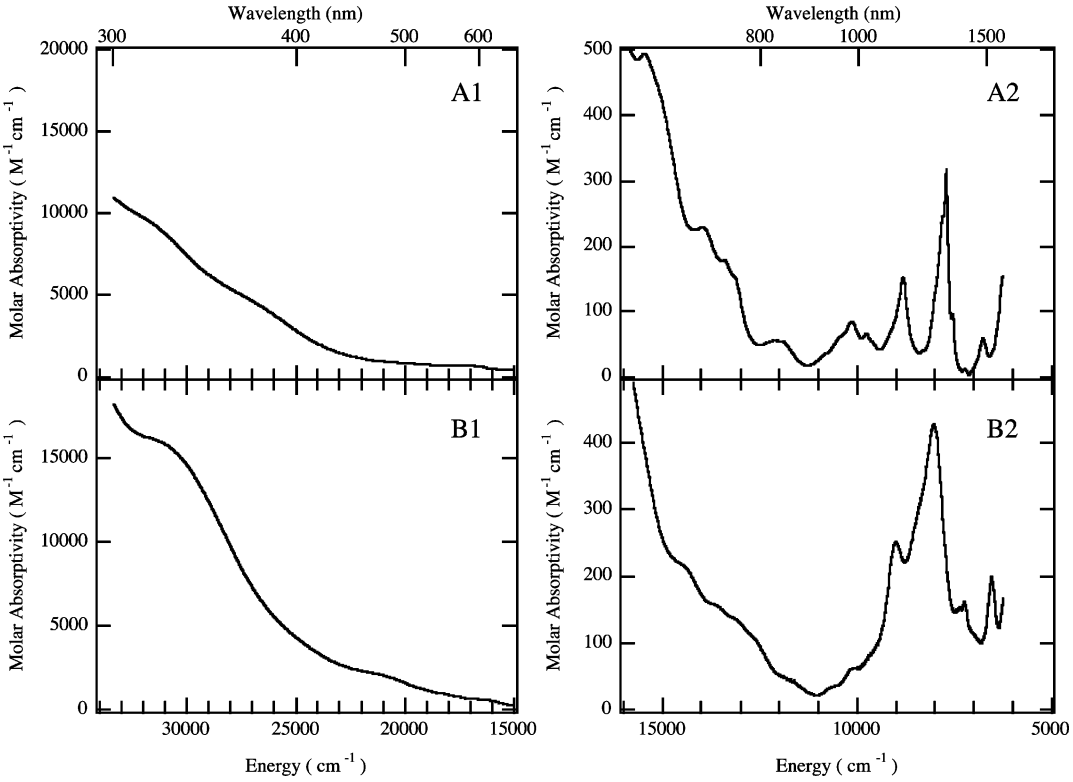

Figure 6. UV−visible−near-infrared electronic absorption spectra for toluene solutions of $(C_5Me_5)_2U^{IV}$ complexes possessing ketimido and imido ligands: (A1 and A2) $(C_5Me_5)_2U[-N{=}C(Ph)_2]_2$ (**10**); (B1 and B2) $(C_5Me_5)_2U(=N\text{-}2,4,6\text{-}{}^tBu_3C_6H_2)$ (**13**).

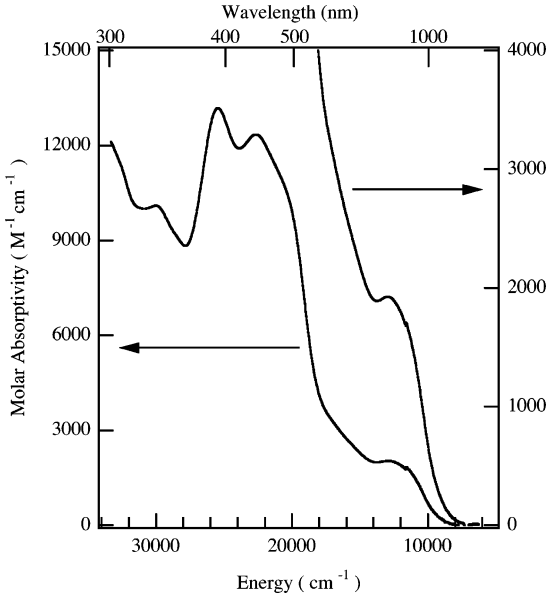

Figure 7. UV−visible−near-infrared electronic absorption spectra for toluene solutions of the hexavalent complex $(C_5Me_5)_2U(=NPh)_2$ (**18**).

those observed for complexes in the first and second classes, and the bands in the higher energy region are comparable in intensity to those in the second class ($\epsilon \approx 10\,000-15\,000\ M^{-1}\ cm^{-1}$), presumably because they arise from similar charge-transfer and ligand-localized $\pi-\pi^*$ and $n-\pi^*$ transitions.

As a final comparative data point, the spectrum for the hexavalent uranium bis(imido) complex (**18**) is provided in Figure 7. As expected for this formally $5f^0$ complex, there are no f−f transitions observed. Instead, the spectrum is dominated by fairly broad, intense ligand-to-metal charge-transfer (LMCT) bands that span the entire spectral window. The structure observed in this spectrum is likely the result of multiple electronic states with vibronic components within each state. Similarly structured spectra have been obtained for virtually all complexes containing the hexavalent UO_2^{2+} moiety, and the origin of the structure in these spectra has been unequivocally assigned to multiple electronic states with vibronic components resolved for most states.[39] The interesting aspect of the spectral behavior of complex **18** is the very low energies to which these charge-transfer transitions extend. Most classical UO_2^{2+} complexes are yellow to orange because the electronic absorption bands are centered in the mid-visible region (∼450−500 nm) and there is little intensity extending to longer wavelengths. In contrast, the absorption intensity is substantial to 1000 nm for the bis(imido) complex, and this broad visible/near-infrared absorbance imparts a dark red-brown color to this complex. Additional room- and low-temperature spectroscopic studies of this complex, including resonance Raman spectroscopy, are underway and will be reported elsewhere.

The intensity variation across the three classes of spectral data sets for the tetravalent uranium complexes is clearly the most interesting and significant aspect of the electronic spectroscopy. Previous studies of the electronic spectral properties of uranium and other actinide metallocenes are very limited in number and have overlooked this important diagnostic criterion.[7−9] As noted above, the intensities in the f−f bands for the first class of complexes (Figure 4, A2−C2) are nominal for actinide complexes having a $5f^2$ electron configuration and reflect the essential Laporte parity forbidden

(39) Denning, R. G. *Struct. Bonding* **1992**, *79*, 215−276.

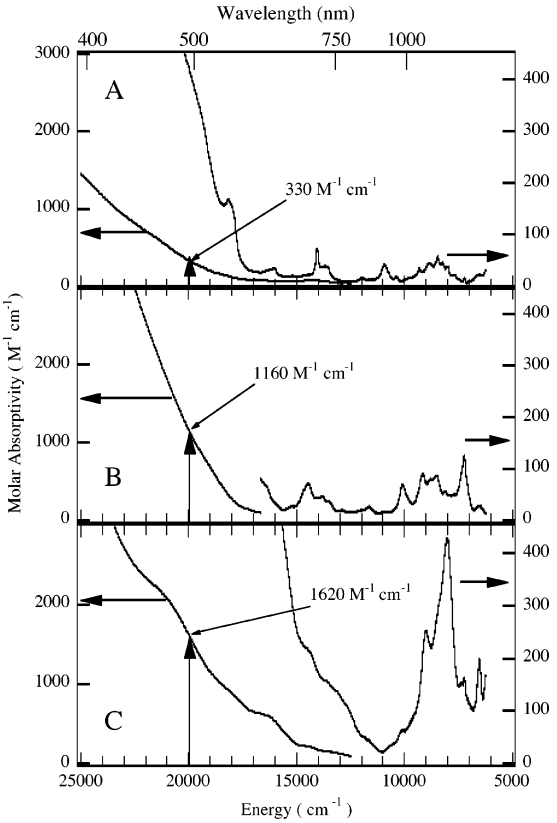

Figure 8. Comparison of UV−visible−near-infrared electronic absorption spectral intensities for a typical complex from each class: (A) class 1, $[(C_5Me_5)_2U(CH_3)_2]$ (**4**); (B) class 2, $(C_5Me_5)_2U[\eta^2(N,N')\text{-}CH_2PhNN{=}CPh_2]_2$ (**9**); (C) class 3, $[(C_5Me_5)_2U[-N{=}C(Ph)_2]_2$ (**10**). The intensity scales are identical for all three sets of spectra to facilitate comparison.

character of these transitions.[34,38] The substantial increase in intensity observed in the f−f bands for the second and third classes suggests the presence of an intensity-generating mechanism not present for the first class of complexes. The term "hypersensitivity" is often used as a catchall to explain unusually large intensities in f−f bands, particularly those in 4f metal complexes.[40] This label, however, is usually reserved to describe only one or a few specific transitions that appear to be associated with and report on deviations from inversion symmetry at the metal center. In the present case, most if not all of the f−f bands progressively gain intensity upon going from the first to the third class of complexes.

The existence, intensity, and energetic proximity of the higher-energy absorption bands in these complexes appear to hold the key to the observed trends in the intensities of the f−f bands. A spectral comparison across the three classes of organouranium(IV) complexes is provided in Figure 8. Here we have arbitrarily chosen the intensity in the higher-energy region at 20 000 cm^{-1} to establish a quantitative comparison, for which the intensity trend is ϵ(class 1) < ϵ(class 2) < ϵ(class 3). This trend persists as the spectral band(s) move to lower energy. As discussed below, the transitions in this lower energy end of the molecular transition region appear to be the most important ones in promoting the f−f intensity enhancement. We propose that the increase in intensity in the f−f bands for the second and third classes of complexes is a direct result of an intensity-stealing mechanism in which the f−f transitions gain intensity by coupling to one or more fully allowed transitions, such as the low-energy charge-transfer transitions observed for the complexes with nitrogen-containing ligands. This type of intensity-stealing mechanism is well-established for the formally Laporte-forbidden d−d transitions of several transition-metal complexes, and it reflects a significant degree of covalency in the bonding between the metal and ligand responsible for the charge-transfer transition.[38] A number of years ago Henrie et al. proposed that covalency in f-element−ligand bonding should be manifest in enhanced intensities in f−f transitions by means of a similar coupling mechanism of the f−f transitions to charge-transfer transitions within the complex.[40] They proposed a framework within which the coupling mechanism might be evaluated on the basis of a simple adaptation of Judd−Ofelt theory for the calculation of the oscillator strength in the f−f bands. The essential features of this formalism are that (1) the mixing occurs between states of the f^n configuration and charge-transfer states of different parity and (2) the intensity enhancement in the f−f bands is directly proportional to the intensity in the charge-transfer transition and inversely proportional to the square of the energetic separation between the charge-transfer state(s) and the f−f state(s). That is, the closer in energy the states, the stronger the coupling and the intensity-stealing process.

The general validity of this intensity-stealing mechanism to account for the intensity enhancement in the f−f bands is supported by the data illustrated in Figure 8. However, this comparison is made over a broad range of complexes for which the charge-transfer states, while clearly present in the second and third classes of complexes, likely have different orbital character and certainly different energies. A more informative and controlled comparison is provided from the series of U(IV) ketimido complexes (**10**−**12**), as shown in Figure 9. These complexes possess very similar molecular structures, and they likely have similar electronic structures. In particular, note that all three complexes have very similar spectra in the f−f region (Figure 9, A2−C2), and all three exhibit significant intensity in the molecular transition region extending to very close energetic proximity with the f−f region. Most important, the intensity variation observed in the f−f bands, while not enormous, tracks closely with the intensity variation seen in the molecular (charge-transfer) bands, as suggested in the formalism of Henrie et al.[40]

A similar comparison might be expected for the two U(IV) hydrazonato complexes (**8**, **9**) illustrated in Figure 5A,B. In fact, while these complexes do clearly exhibit the f−f intensity enhancement relative to the σ-donor complexes (Figures 4 and 8), there is practically no difference in the intensities of either the f−f bands or the molecular transitions between the benzyl-substituted bis(hydrazonato) complex (**9**) and methyl-substituted bis(hydrazonato) complex (**8**). The diminished extent of f−f intensity enhancement in these hydrazonato complexes compared to that in the complexes in the third class (ketimides (**10**−**12**) and imide (**13**)) most likely reflects the greater energy separation between the

(40) Henrie, D. E.; Fellows, R. L.; Choppin, G. R. *Coord. Chem. Rev.* **1976**, *18*, 199−224.

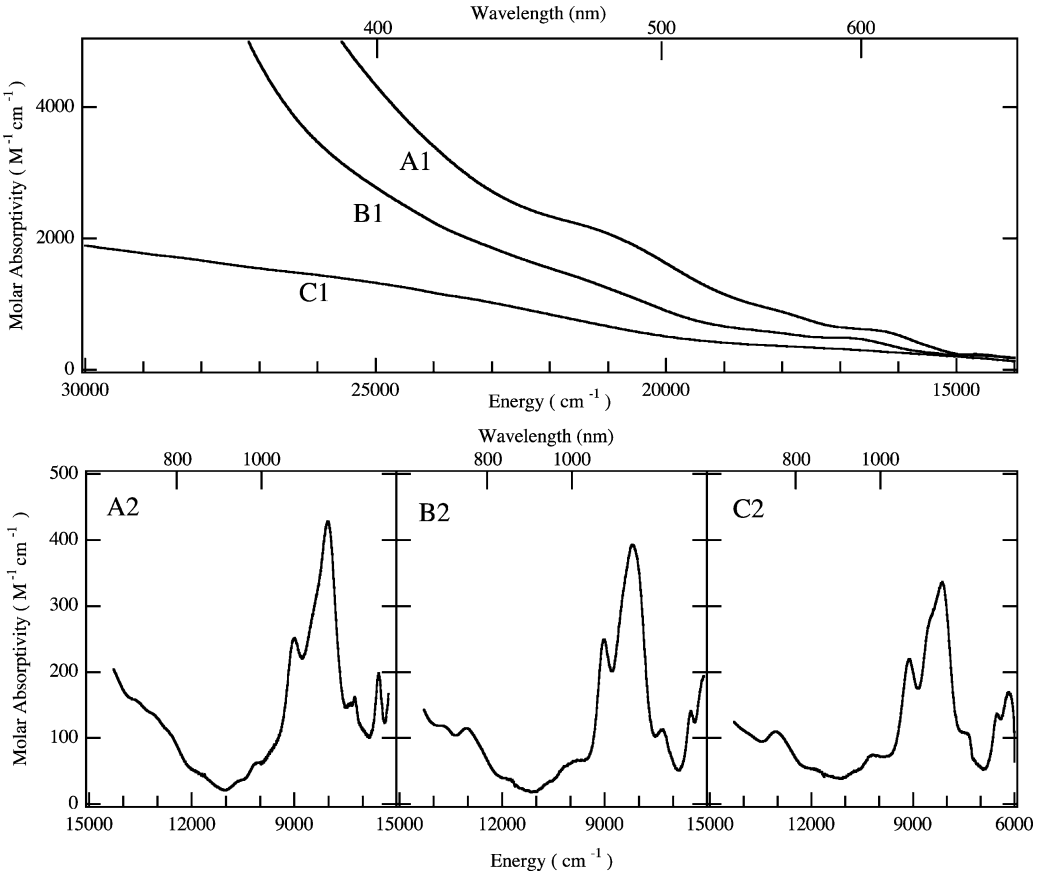

Figure 9. Comparison of UV−visible−near-infrared electronic absorption spectral intensities for the $(C_5Me_5)_2U^{IV}$ ketimido complexes: (A1 and A2) $(C_5Me_5)_2U[-N{=}C(Ph)_2]_2$ (**10**); (B1 and B2) $(C_5Me_5)_2U[-N{=}C(Ph)(CH_2Ph)]_2$ (**12**); (C1 and C2) $(C_5Me_5)_2U[-N{=}C(Ph)(CH_3)]_2$ (**11**). The intensity scales are identical for all three sets of spectra to facilitate comparison.

f−f states and the charge-transfer state(s) in the hydrazonato complexes. While specific state assignments have not yet been made for either the hydrazonato or ketimido complexes to establish the relative energetic positions of $\pi-\pi^*$ and charge-transfer states, there is no question that the spectral intensity of these molecular states extends to much lower energy for the ketimido complexes than for the hydrazonato complexes (Figure 8). We also have very recent resonance Raman spectroscopic data for the U(IV) ketimido complexes (**10**−**12**) that substantiate a charge-transfer assignment for these lowest energy molecular electronic transitions.[41]

Conclusions

It is clear that incorporation of nitrogen-donor ligands into uranium metallocene complexes provides for much richer electronic structural properties compared to those observed in analogous complexes possessing only halide or alkyl groups. In particular, the pentavalent metal oxidation state is substantially stabilized and f−f transition intensities are greatly enhanced as a result of the incorporation of the nitrogen-bearing ligands. These nitrogen-containing ligands contribute energetically low-lying orbitals that (1) provide a mechanism for enhancing covalent metal−ligand interactions involving the metal 5f orbitals and (2) introduce low-energy charge-transfer transitions that, due to their energetic proximity to the f−f states of U(IV), lend added intensity to the f−f transitions. Thus, the f−f band intensities provide a direct measure of the degree of covalent interaction between the metal f orbitals and the ancillary ligand orbitals. The strong intensities of the f−f bands in the uranium(IV) ketimides and imide reflect the fact that the charge-transfer transitions for these complexes extend to much lower energy and can therefore interact more strongly with the f−f states.

(41) Da Re, R. E.; Jantunen, K. C.; Golden, J. T.; Kiplinger, J. L.; Morris, D. E. Manuscript in preparation, 2004.

Experimental Section

Syntheses. (a) General Procedures. Reactions and manipulations were performed at 20 °C in a recirculating Vacuum Atmospheres Model HE-553-2 inert-atmosphere (N_2 or He) drybox with a MO-40-2 Dri-Train, or using standard Schlenk and high-vacuum-line techniques. Glassware was dried overnight at 150 °C before use.

(b) Materials. Unless otherwise noted, reagents were purchased from commercial suppliers and used without further purification. Anhydrous toluene (Aldrich) and tetrahydrofuran (Aldrich) were passed through a column of activated alumina (A2, 12 × 32, Purify) under nitrogen and stored over activated 4 Å molecular sieves prior to use. $(C_5Me_5)_2UCl_2$ (**1**),[21] $(C_5Me_5)_2U(CH_2Ph)_2$ (**2**),[21] $(C_5Me_5)U(CH_2Ph)_3$ (**3**),[17] $(C_5Me_5)_2U(CH_3)_2$ (**4**),[21] $(C_5Me_5)_2U(CH_3)(SO_3CF_3)$ (**5**),[18] $(C_5Me_5)_2U(\eta^2(N,N')\text{-}CH_3NN{=}CPh_2)(SO_3CF_3)$ (**6**),[18] $(C_5Me_5)_2U(\eta^2(N,N)\text{-}CH_3NN{=}CPh_2)(Cl)$ (**7**),[18] $(C_5Me_5)_2U(\eta^2(N,N')\text{-}CH_3NN{=}CPh_2)_2$ (**8**),[22] $(C_5Me_5)_2U(\eta^2(N,N')\text{-}CH_2PhNN{=}CPh_2)_2$ (**9**),[22] $(C_5Me_5)_2U[-N{=}C(Ph)(R)]_2$ (R = Ph (**10**),[19] CH_3 (**11**),[23] CH_2Ph (**12**)),[23] $(C_5Me_5)_2U(=N\text{-}2,4,6\text{-}{}^tBu_3C_6H_2)$ (**13**),[42] $(C_5Me_5)_2Th(\eta^2(N,N')\text{-}PhNN{=}CPh_2)_2$ (**14**),[22] $(C_5Me_5)_2Th(\eta^2(N,N')\text{-}CH_2PhNN{=}CPh_2)_2$ (**15**),[22] $(C_5Me_5)_2Th[-N{=}C(Ph)_2]_2$ (**16**),[23] $(C_5Me_5)_2Th[-N{=}C(Ph)\text{-}$

$(CH_2Ph)]_2$ (**17**),[23] and $(C_5Me_5)_2U(=NPh)_2$ (**18**)[42] were prepared according to literature procedures.

Electronic Spectroscopy. Electronic absorption spectral data were obtained for toluene solutions of all complexes over the wavelength range from 300 to 1600 nm on a Perkin-Elmer Model Lambda 19 UV−visible−near-infrared spectrophotometer. All data were collected in 1 cm path length quartz cuvettes modified to incorporate a Schlenk-type sealable joint. Cells were loaded in an inert-atmosphere glovebox and run versus a toluene reference. Strong absorption bands from overtone vibrations of the toluene solvent precluded the collection of data at wavelengths longer than 1600 nm, but samples were run separately versus air references to ensure that the observed absorption bands were attributable to the complexes and not the solvent. All uranium complex samples were run at two dilutions, typically ∼0.1 and ∼0.5 mM, to optimize absorbance in the UV−visible and near-infrared regions, respectively. Spectral resolution was typically 2 nm in the visible region and 4−6 nm in the near-infrared region.

Electrochemistry. Cyclic voltammetric data were obtained in the Vacuum Atmospheres glovebox system described above. All data were collected using a Perkin-Elmer Princeton Applied Research Corp. (PARC) Model 263 potentiostat under computer control with PARC Model 270 software. All sample solutions were ∼5 mM in complex with 0.1 M $[(n\text{-}C_4H_9)_4N][B(C_6F_5)_4]$ supporting electrolyte in THF solvent. This electrolyte has been shown previously to greatly diminish the solution resistance in low-dielectric solvents such as THF. Nonetheless, all data were collected with the positive-feedback *iR* compensation feature of the software/potentiostat activated to ensure minimal contribution to the voltammetric waves from uncompensated solution resistance (typically ∼1 kΩ under the conditions employed). Solutions were contained in PARC Model K0264 microcells consisting of an ∼3 mm diameter Pt-disk working electrode, a Pt-wire counter electrode, and a silver-wire quasi-reference electrode. Scan rates from 20 to 5000 mV/s were employed to assess the chemical and electrochemical reversibility of the observed redox transformations. Potential calibrations were performed in situ for all samples at the end of each data collection cycle by addition of ferrocene and the use of the ferrocenium/ferrocene couple as an internal potential standard.

Both electronic absorption and cyclic voltammetric data were analyzed using Wavemetrics IGOR Pro (Version 4.0) software on a Macintosh platform.

Acknowledgment. Support for this research was provided by the United States Department of Energy, Office of Science, Office of Basic Energy Science, under the auspices of the Heavy Element Chemistry Program and the Los Alamos National Laboratory's Laboratory Directed Research and Development Office. K.C.J. and I.C.-R. acknowledge fellowship support from the G. T. Seaborg Institute for Transactinium Science at Los Alamos. J.L.K. acknowledges support as a Fredrick Reines Postdoctoral Fellow at Los Alamos during the initial stages of this work. This research was performed at Los Alamos National Laboratory under contract with the University of California (Contract No. W-7405-ENG-36).

OM049634V

(42) Arney, D. S. J.; Burns, C. J. *J. Am. Chem. Soc.* **1995**, *117*, 9448−9460.